Supporting Information

Facile Synthesis of $BaCeO_3$@g-C_3N_4 n-type Semiconductor Heterojunctions for Green Hydrogen Production via Multimodal Photo and Electro-catalytic Pathways

Shireen Khan[1,2], Syed Asim Ali[1,3], Amna Khatoon[2], Bhawna Rawat[4], Kamalakannan Kailasam[4] and Tokeer Ahmad[1*]

[1]Nanochemistry Laboratory, Department of Chemistry, Jamia Millia Islamia, New Delhi-110025, India

[2]Department of Environmental Science, Jamia Millia Islamia, New Delhi 110025, India

[3]Interdisciplinary Research Center for Hydrogen Technologies and Carbon Management (IRC-HTCM), King Fahd University of Petroleum and Minerals (KFUPM), Dhahran-31261, Saudi Arabia

[4]Institute of Nano Science and Technology (INST), Knowledge City, Sector 81, SAS Nagar, Manauli PO, 140306 Mohali, Punjab, India

Address for Correspondence:

E-mail: tahmad3@jmi.ac.in; Phone: 91-11-26981717, Extn: 3261

Chemicals and Solvents:

Chemicals used were barium nitrate ($Ba(NO_3)_2$, 99.0%), cerium nitrate ($Ce(NO_3)_2$, alfa aesar, 99.5%), Melamine (Alfa Aesar), citric acid (Merck, 99%), ethylene glycol (Merck, 99%), hydrochloric acid (Merck, 37%), acetic acid glacial (SRL, 99%), acetone (Merck) and ethanol (Merck). While double-distilled water was utilized to prepare all of the solutions with no further purifications.

Characterization Techniques:

For the determination of structural and morphological properties of pristine $BaCeO_3$, g-C_3N_4 and their heterostructures, the X-ray diffraction (XRD), (RigakuUltima-IV, Cu-Kα irradiation having λ=1.5416 Å), Field emission-scanning electron microscope (FE-SEM) (NOVA Nano SEM 450, 20 kV), FEI energy-dispersive X-ray (EDX) and high resolution-transmission electron microscope (HR-TEM) (Thermo scientific-TALOS instrument, 200 kV) were employed. Quantachrome® ASiQwin™ - Automated Gas Sorption Data to evaluate the BET surface area and pore size distribution of as-synthesized nanostructures. Perkin Elmer-365 spectrophotometer and fiber-optic spectrometer equipped with Olympus BX-51 microscope were used for investigating optical studies. X-ray photoelectron spectroscopy (XPS) was utilized via PHI 5000 VersaProbe II XPS system for understanding the electronic properties of as-synthesized nanostructures.

Photocatalytic H_2 Evolution Studies:

Photocatalytic hydrogen production experiments were performed in the photocatalytic reactor, which comprised a cylindrical quartz cell with a dedicated opening site where rubber septum was placed. In the standard reaction process, 20 mg of as-synthesized nanostructures were stirred in 50 mL of water alongside a considerable quantity of equimolar Na_2S and Na_2SO_3 which acted as the sacrificial electron donors. The photocatalytic reaction solution was exposed to N_2 at high pressure to eliminate any foreign impurity and to provide inertial condition. Followed by which photo-reactor was placed 10 cm away from light simulator (200 W, Hg-Xe arc lamp, 450 nm band pass filter, Newport, USA). Produced H_2 was evaluated by sampling in the 1 h time period via gas chromatograph, Perkin Elmer, Clarus 590 GC equipped with thermal conductivity detector (TCD).

Apparent Quantum Yield (AQY) Measurements:

AQY of as-prepared $BaCeO_3$ and g-C_3N_4 and their heterostructures was evaluated during the photocatalytic operations by employing the general formula:

$$\text{AQY \%} = \frac{2\ X\ numbers\ of\ evolved\ H_2\ molecule}{numbers\ of\ incident\ photons\ \ (N_{photon})} \text{ X 100}$$

$$\mathbf{N_{photon}} = \frac{PA\lambda t}{hc}$$

Where P denotes the power of light source employed for photocatalytic reactions (0.113 W/cm^2), A represents an illuminating area (16.62 cm^2), λ is the wavelength of the light during photocatalysis (450 nm), t denotes the time span of photocatalytic run, h is the plank's constant (6.626 x 10^{-34} J s) and c is the speed of light (3 x 10^8 m/s).

Electrochemical H_2 Evolution Studies:

Electrochemical studies were carried out to realize the multi-functionality of as-fabricated nanostructures towards HER applications. In the typical three-electrode system, the cathodic and anodic current densities were measured as a function of H_2 evolution, respectively. The working electrode was prepared by coating the homogeneous layer of electrocatalyst dispersed in ethanol/Nafion solution on Indium-doped Tin oxide (ITO) 1cm^2, whereas the platinum coil and calomel electrodes acted as counter and reference electrodes, respectively. Electrochemical measurements were recorded on an Autolab PGSTAT204 setup. Linear sweep voltammetry (LSV) polarization curves and cyclic voltammetry (CV) plots were obtained at a 100 mV/s scan rate.

Photo-Electrochemical H_2 Evolution Studies:

In order to investigate the photo-electrocatalytic response of pristine $BaCeO_3$, g-C_3N_4, and their heterostructures, photo-electrochemical studies were carried out on an Autolab PGSTAT204 setup, Electrochemical Workstation equipped with a Potentiostat, by employing a photo-electroactive material-coated ITO 1cm^2, Pt wire, and calomel electrode as the working, counter, and reference electrodes. 1 mg as synthesized nanostructures dispersed in isopropyl alcohol and Nafion were coated on ITO. The electrochemical setup consisting of a 0.5 M H_2SO_4 electrolytic solution was stationed near a light simulator (50 W, Hg-Xe arc lamp, quartz tungsten halogen, Newport, USA) solar simulator, and various responses were examined thereafter.

Photoluminescence and Time Resolved Photoluminescence Spectroscopy:

Photoluminescence (PL) and time-resolved PL of all of the samples were collected using an Edinburgh Instruments FLSP920. The spectra of PL lifespan decay were recorded using the time-correlated single photon counting (TCSPC) technique. A 434 nm pulsed laser diode was employed for the lifespan evaluations of each material. To begin with, the powder samples were sonicated for 10 minutes in 2 mL of isopropyl alcohol (IPA). Concentrated solutions were produced in advance and dropped onto glass surfaces in preparation for the collection of PL data. The rate constant for the heterostructure electron transfer reaction (K_{et}) were derived using the following equation after biexponential fitting of all the measurement data:

$$K_{et} = \frac{1}{\tau_{avg}}$$

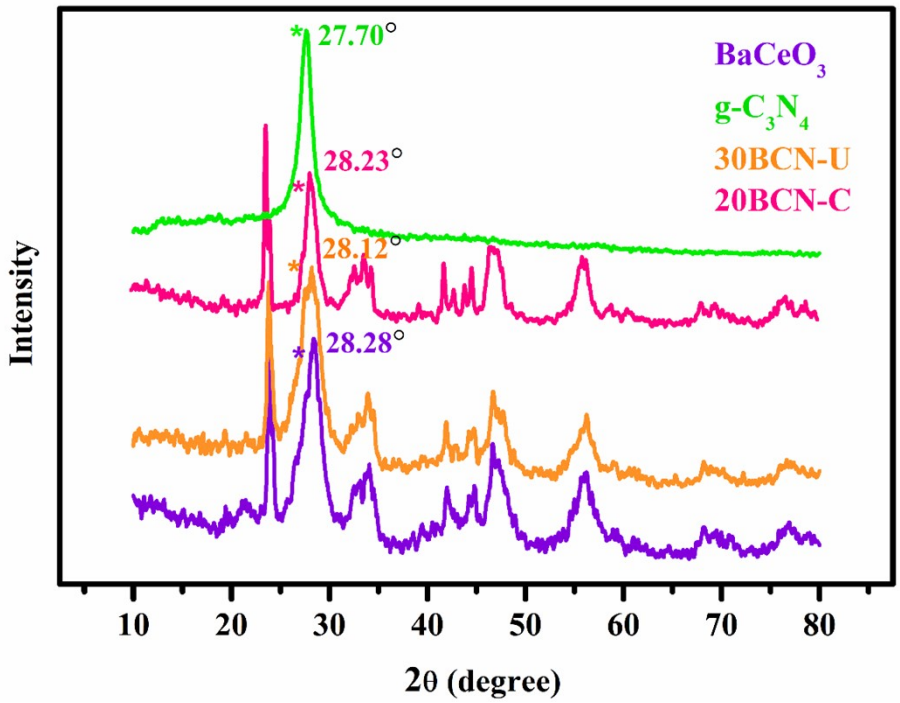

Figure S1. Peak shifting of $BaCeO_3$ (002) plane in 30BCN-U and 20BCN-C heterostructures.

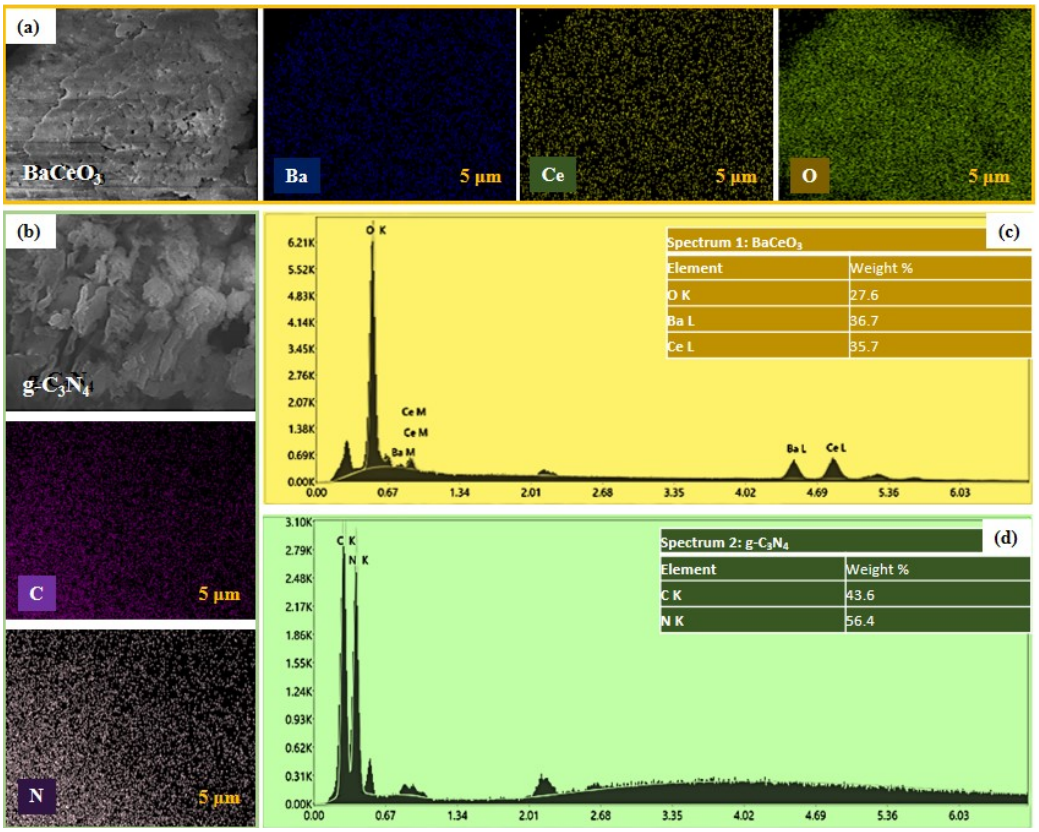

Figure S2. EDAX analysis of (a, c) $BaCeO_3$ and (b, d) g-C_3N_4.

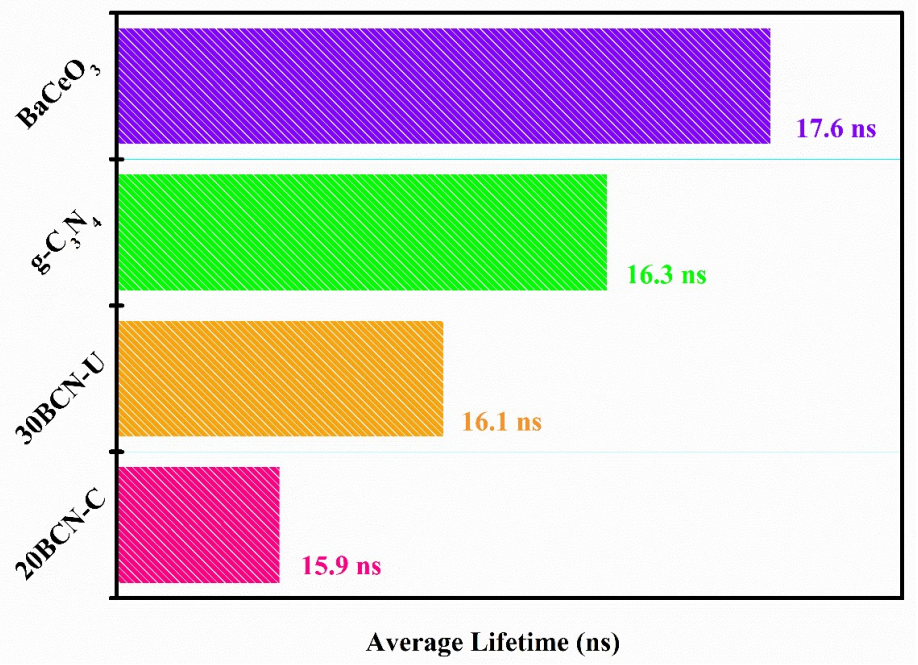

Figure S3. Time-resolved average lifetime for BCO, CN, 30BCN-U, and 20BCN-C.

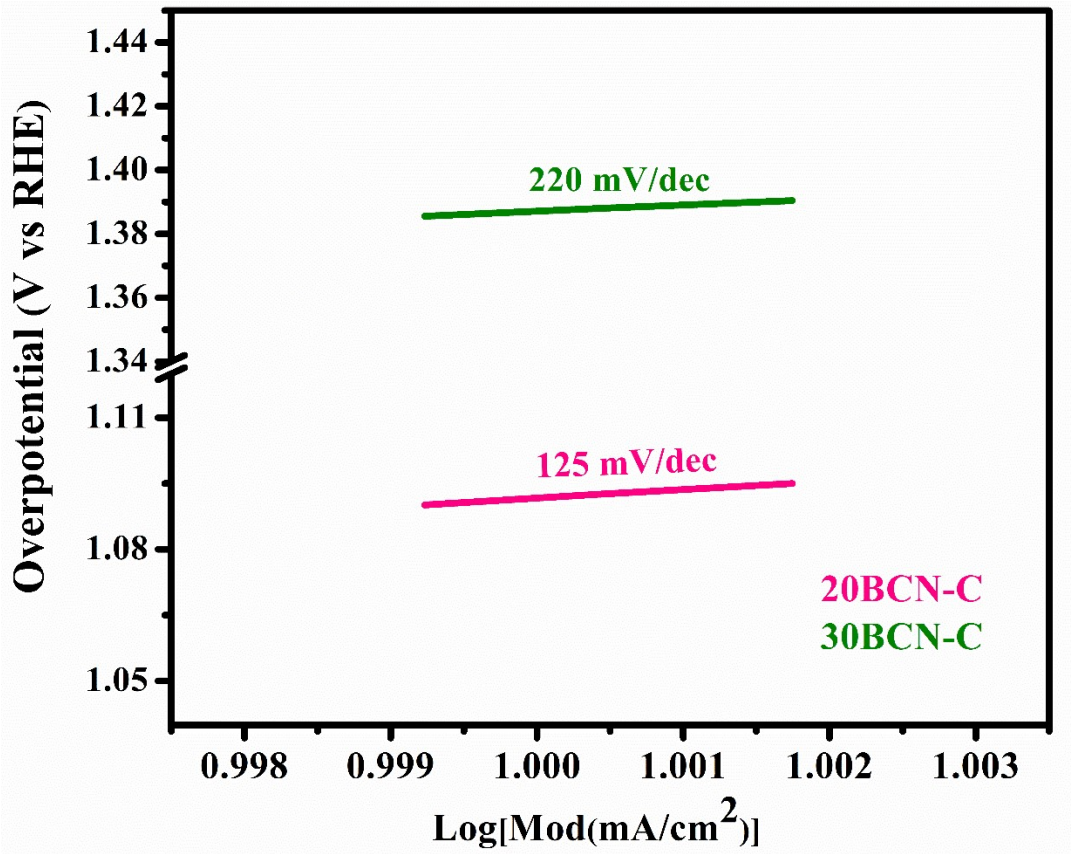

Figure S4. Tafel plot of 20BCN-C and 30BCN-C heterostructures.

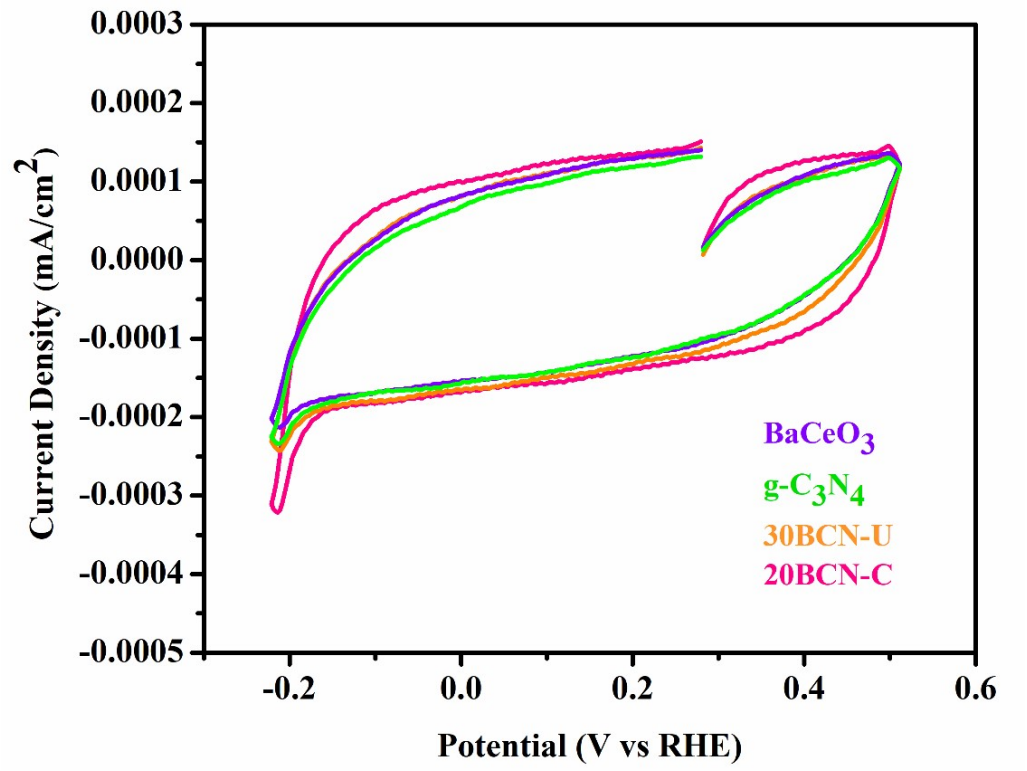

Figure S5. Electrocatalytic CV plot of as-prepared electrocatalysts.

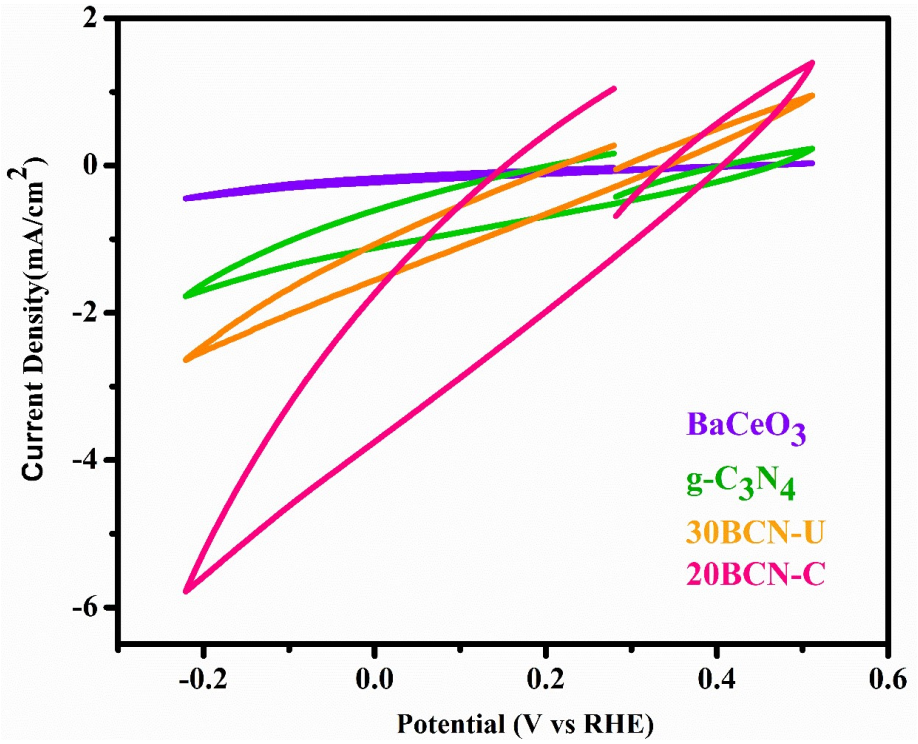

Figure S6. PEC-CV plot of as-prepared catalytic systems.

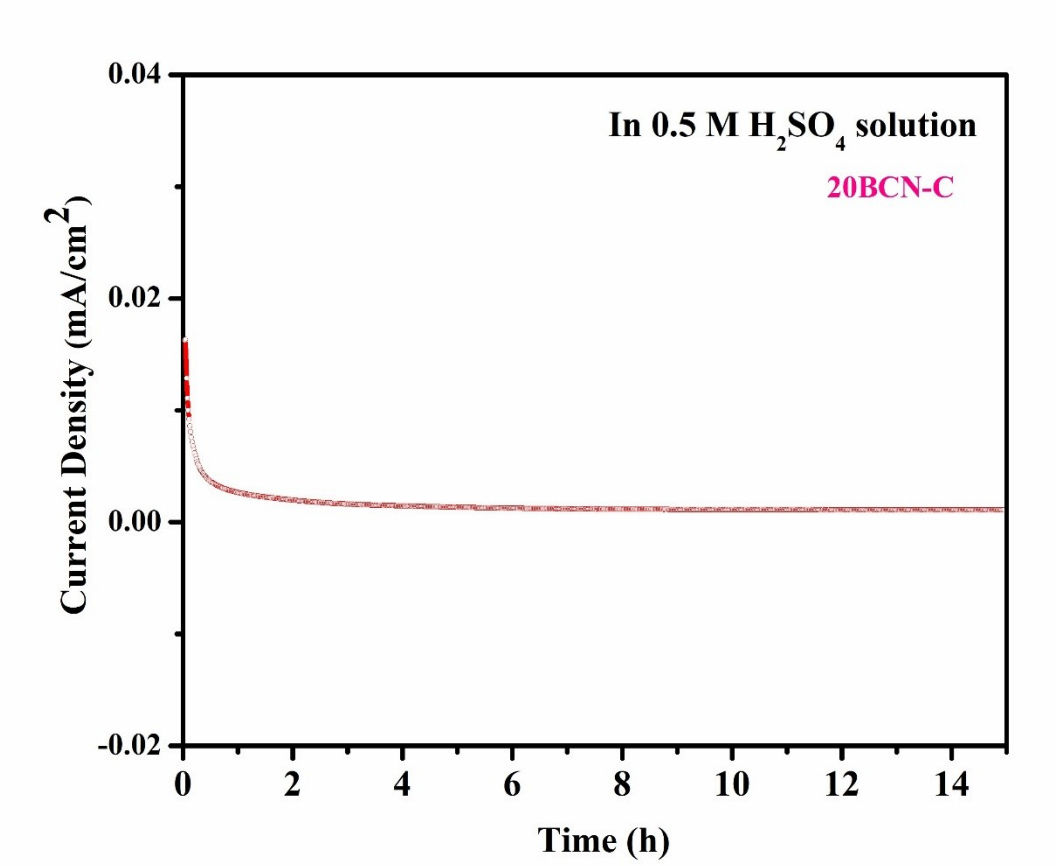

Figure S7. Chronoamperometric test of 20BCN-C.

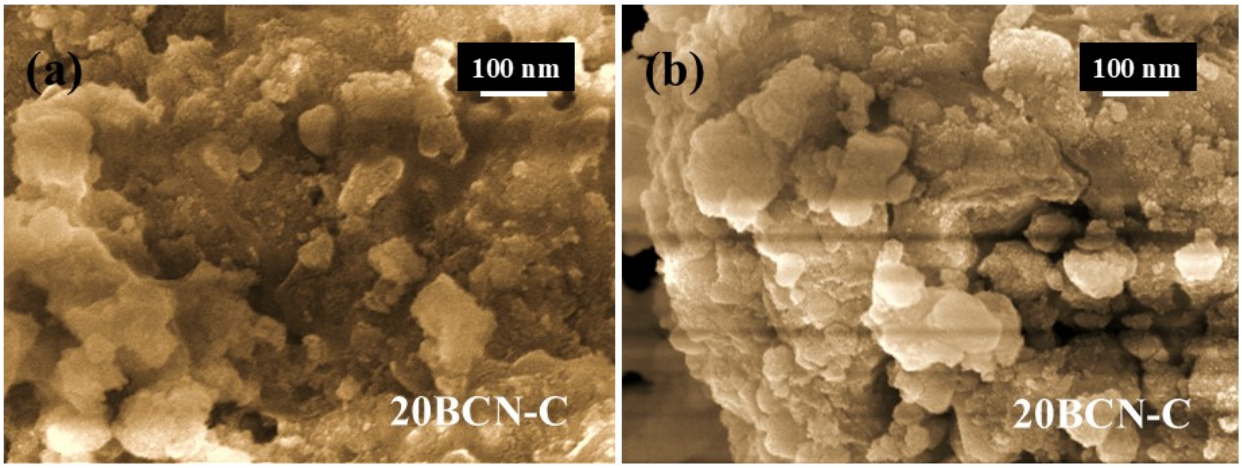

Figure S8. SEM images of 20BCN-C after (a) photocatalysis, and (b) electrocatalysis

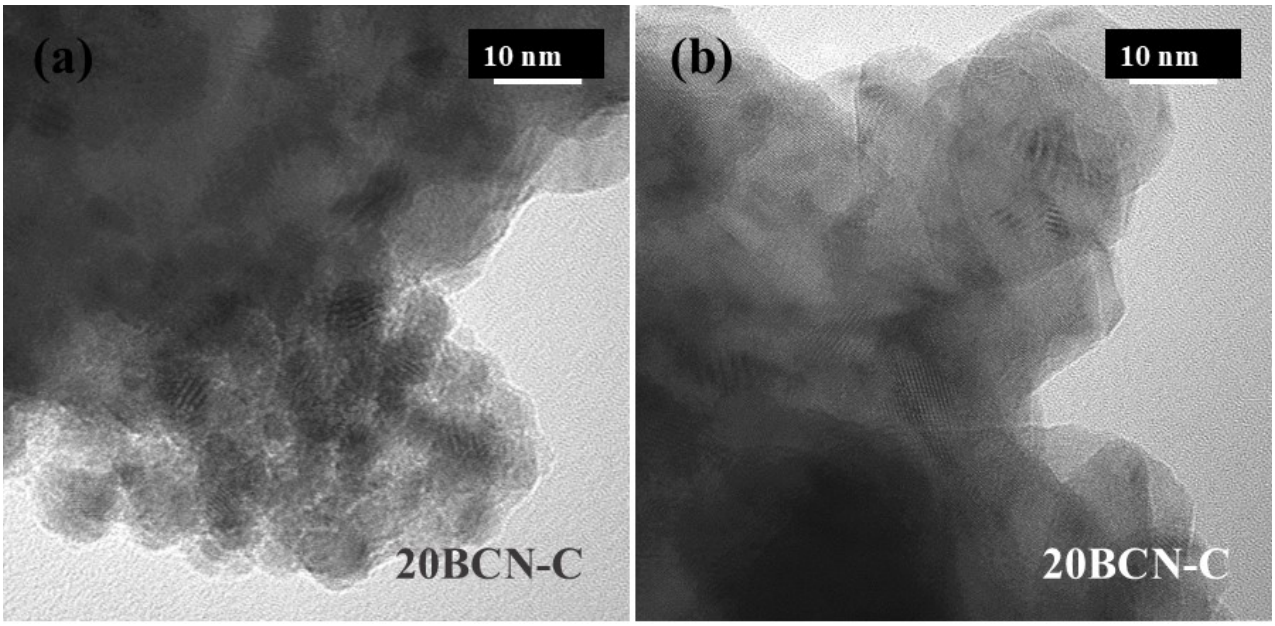

Figure S9. HR-TEM images of 20BCN-C after (a) electrocatalysis and (b) photocatalysis.

Table S1. Exponential charge-transfer dynamics of $BaCeO_3$, g-C_3N_4, 30BCN-U, and 20BCN-C.

Materials	τ_1 (ns)	α_1	τ_2 (ns)	α_2	τ_3 (ns)	α_3	τ_{avg}	**K_{et}** (10^{-9} s^{-1})
BCO	2.4	27.61	6.9	51.19	0.2	21.20	17.6	-
CN	5.7	56.28	1.6	18.96	0.2	24.75	16.3	-
30BCN-U	6.0	55.54	1.7	20.95	0.2	23.51	16.1	0.06
20BCN-C	1.6	27.35	5.7	51.47	0.2	21.18	15.9	0.06

Table S2. Photocatalytic hydrogen evolution for both pure and all as-prepared heterostructures.

Materials (Sacrificial Agent: Na_2S/Na_2SO_3)	**Band Gap (eV)**	**Photocatalytic Hydrogen Evolution (mmol/g_{cat}/h)**
$BaCeO_3$	2.89	6.45
g-C_3N_4	2.64	7.84

10BCN-U	2.85	8.74
20BCN-U	2.8	9.30
30BCN-U	2.79	10.01
10BCN-C	2.78	14.24
20BCN-C	2.69	15.21
30BCN-C	2.76	15.07

Table S3. Correlative Study of electrocatalytic (EC) and photoelectrocatalytic (PEC) activity of all prepared materials.

Materials (Electrolyte: 0.5 M H_2SO_4	**Current Density (mA/cm^2)**	**EC-Over-potential (mV)**	**Tafel HER (mV/dec)**	**Current Density (mA/cm^2)**	**PEC-Over-potential (mV)**	**Tafel HER (mV/dec)**
$BaCeO_3$	-1.00	-	-	-2.77	-	-
g-C_3N_4	-5.12	-	-	-70.69	-1.02	224
10BCN-U	-5.33	-	-	-74.68	-1.01	210
20BCN-U	-5.71	-	-	-77.13	-1.00	206
30BCN-U	-6.29	-	-	-65.81	-1.00	206
10BCN-C	-7.21	-	-	-71.07	-1.00	206
20BCN-C	-13.60	-1.09	125	-75.42	-2.06	95
30BCN-C	-15.86	-1.38	220	-74.58	-0.99	112